Published in final edited form as:
FEBS Lett. 2007 February 20; 581(4): 644–650.

Myosin 1E interacts with synaptojanin-1 and dynamin via its SH3 domain

Mira Krendel[1,#], **Emily K. Osterweil**[1,2], and **Mark S. Mooseker**[1,3,4]
1*Departments of Molecular, Cellular, and Developmental Biology, Yale University, New Haven, CT 06511*

3*Departments of Cell Biology, Yale University, New Haven, CT 06511*

4*Departments of Pathology, Yale University, New Haven, CT 06511*

Abstract

Myosin 1E is one of two “long-tailed” human Class I myosins that contain an SH3 domain within the tail region. SH3 domains of yeast and amoeboid myosins I interact with activators of the Arp2/3 complex, an important regulator of actin polymerization. No binding partners for the SH3 domains of myosins I have been identified in higher eukaryotes. In the current study, we show that two proteins with prominent functions in endocytosis, synaptojanin-1 and dynamin, bind to the SH3 domain of human Myo1E. Myosin 1E colocalizes with clathrin- and dynamin-containing puncta at the plasma membrane and this co-localization requires an intact SH3 domain. Expression of Myo1E tail, which acts in a dominant-negative manner, inhibits endocytosis of transferrin. Our findings suggest that myosin 1E may contribute to receptor-mediated endocytosis.

Keywords

myosin; dynamin; synaptojanin; endocytosis; SH3 domain

INTRODUCTION

Class I myosins are actin-dependent molecular motors expressed in various organisms from yeast to humans. All class I myosins contain a head (motor) domain, a light chain-binding neck domain, and a tail, which can be either short, consisting only of a membrane-binding tail homology (TH)-1 domain, or long, with a proline-rich TH2 domain and an SH3 domain in addition to TH1. In humans and mice, there are eight myosin I (Myo1) heavy chain genes, two of which, Myo1E and F, are long tailed [1,2].

Long-tailed Myo1s are found in both lower and higher eukaryotes. Long-tailed yeast and amoeboid Myo1s interact with activators of the Arp2/3 complex, an important regulator of actin polymerization, and are involved in actin reorganization and endocytosis [3-9]. In budding yeast, inactivation of Myo1 isoforms (Myo3p and Myo5p) leads to defects in endocytosis [3]. In *Acanthamoeba*, various Myo1 isoforms are found in association with

[2]Current address - The Picower Institute for Learning and Memory, Massachusetts Institute of Technology, Cambridge, MA, 02139
[#]Corresponding author. PO Box 208103, KBT-342, 266 Whitney Ave., New Haven, CT 06520-8103, Tel.: (203) 432-3469. Fax: (203) 432-6161. E-mail: mira.krendel@yale.edu

intracellular vesicles [10]. In *Dictyostelium*, long-tailed Myo1s (myo B, C, and D) are required for fluid-phase endocytosis [11].

Myo1e, the mouse homolog of the human long-tailed myosin, Myo1E (formerly referred to as Myo1C under the old myosin nomenclature [12]), has been previously localized to phagocytic structures [13]. In this study, we report that Myo1E binds to two proline-rich proteins, synaptojanin-1 and dynamin, via its SH3 domain, and can be observed to co-localize with dynamin by immunofluorescence microscopy. Synaptojanin-1 and dynamin are involved in clathrin-mediated endocytosis, and our observations of live cells using total internal reflection fluorescence microscopy microscopy (TIRF) indicate that Myo1E colocalizes with clathrin- and dynamin-containing puncta at the plasma membrane. Expression of Myo1E tail, which acts in a dominant-negative manner, inhibits endocytosis of transferrin, which suggests that interaction of Myo1E with endocytic proteins may play an important role in receptor-mediated endocytosis.

MATERIALS AND METHODS

Materials

Antibodies: rabbit anti-Myo1E [14], mouse monoclonal anti-myc (Zymed), rabbit anti-dynamin-2 (Oncogene), mouse anti-dynamin Hudy-1 (Upstate), anti-GFP (Molecular Probes). Secondary antibodies labeled with Alexa-488 and -568 were purchased from Molecular Probes.

Cloning and recombinant protein expression

All constructs were produced using PCR cloning and vectors pEGFP-C1 and pLNCX2-EGFP (BD Biosciences Clontech). Primers used to subclone Myo1E tail (including TH1, TH2, and SH3 domains) flank AA 710-1109, primers for subcloning TH1 domain surround AA 717-920, TH2 domain – AA 913-1060, TH3 domain - AA 1052-1109. GST-tagged proteins were expressed using vector pGEX-5X-3 and affinity-purified according to standard protocols. HeLa and Cos-1 cells were cultured in DMEM supplemented with 10% fetal bovine serum (FBS) and transfected using Lipofectamine.

Yeast two-hybrid screening

A Myo1E tail fragment (TH2+SH3) subcloned into pGBKT7-BD vector using primers flanking aa 915-1109 was used to screen pretransformed human kidney Matchmaker cDNA library (Clontech) following the manufacturer's protocol. Positive clones were isolated and verified by mating with yeast strains containing empty vector, lamin C (negative control), or Myo1E bait construct (see Fig. 1). Synaptojanin-1 fragment identified using yeast two-hybrid represents a splice form that has previously been isolated from embryonic muscle cells (Genbank accession number **DQ421853.1**).

Binding and immunoprecipitation assays

Pull-down of proteins from rat brain extracts was performed as described [15]. For pull-downs from HeLa or Cos-1 cells, cells were lysed in 20 mM imidazole (pH 7.2), 75 mM KCl, 1 mM EGTA, 2.5 mM $MgCl_2$, 1% NP-40 and centrifuged for 15 min. at 16,000 g. The supernatant was incubated with GST-tagged proteins and glutathione agarose for 3 hrs at 4°C. Beads were washed 4 times with phosphate-buffered saline containing 1% Triton X-100.

Synaptojanin-1 and dynamin were purified from rat brain essentially as described [16] except that 20 mM Pipes pH 6.5, 1.2 M NaCl, 1 mM EDTA was used to elute bound dynamin and synaptojanin-1 from endophilin-SH3-beads and a Source 15Q FPLC column (Amersham) eluted with a linear gradient from 0 to 0.3 M NaCl was used to separate dynamin from synaptojanin-1. For *in vitro* binding assays, purified proteins and glutathione agarose beads

were incubated for 2 hrs at 4°C. The bead pellets and unbound proteins were separated by centrifugation and processed for SDS-PAGE.

Deoxycholate-solublized, synapse-enriched rat brain extracts were prepared essentially as described [17]. Extracts were pre-cleared with 1/10 volume protein-A-Sepharose (Amersham) 1 hr at 4°C, and incubated with 100 μg/ml anti-Myo1E antibody or rabbit IgG overnight at 4° C. Protein-A-Sepharose (blocked with 5% BSA) was added at 1/10 dilution, and incubated 1 hr at 4°C. Pellets were washed 7×5 min with 10 mg/L BSA, 1 mM DTT, 1 mM EGTA, 0.2 M KCl, 5 mM Mg-ATP, 1 mM Pefabloc, 50 mM Tris pH 7.4, 0.1% Triton X-100, and processed for SDS-PAGE.

TIRF microscopy

Swiss3T3 cells stably expressing DsRed-clathrin were cultured in DMEM/10% FBS the presence of 0.5 mg/ml G-418. Cells were transiently transfected with EGFP-tagged myosin constructs using 3.4 μg total DNA and 10 μl Lipofectamine 2000 per 35 mm dish. For analysis of dynamin and Myo1E localization, untransfected Swiss3T3 cells were transiently transfected with EGFP-Myo1E and mRFP-dynamin-1 as described above. Cells were trypsinized and replated onto 35-mm glass-bottom dishes (Well-Co, Warner Instruments, Hamden, CT) 3 hrs post-transfection and imaged the following day using a Nikon Eclipse 2000 multimode TIRF microscope prototype. During imaging cells were maintained in DMEM containing 25 mM HEPES and no phenol red supplemented with 5% FBS, using a dish warmer (Warner Instruments) to maintain 37°C temperature. For analysis of Myo1E and clathrin colocalization, green and red channels for a single frame from each time-lapse movie were examined separately using ImageJ, and each distinct fluorescent punctum was manually marked. The two sets of marked images were then superimposed, and puncta that appeared in both channels, as well as puncta that were present only in the red or only in the green channels, were counted. At least three separate dishes of cells were examined for each construct.

Transferrin internalization

Internalization assays using Alexa-568-transferrin were performed as described [18] except that PBS (pH 4) was used in place of citrate buffer to remove surface-bound transferrin. Image collection was performed using Bio-Rad 1024 confocal microscope. For the analysis of transferrin uptake in cells expressing EGFP-tagged Myo1E tail constructs, images of at least 100 EGFP-expressing cells were collected for each construct, and cells that exhibited punctate transferrin labeling were counted as positive and cells that did not contain distinct transferrin puncta counted as negative.

Immunofluorescence microscopy

For immunofluorescence staining, cells were plated onto acid-washed coverslips and fixed using pH-shift fixation as described in [19]. Anti-Myo1E polyclonal antibody and Hudy-1 monoclonal antibody were used to label Myo1E and dynamin, respectively.

RESULTS

Identification of synaptojanin-1 as a Myo1E-binding protein using yeast two-hybrid screening

The tail of Myo1E contains a positively charged TH1 domain, a proline-rich TH2 region, and an SH3 domain, which may interact with proline-rich motif-containing proteins (Figure 1A). To identify proteins binding to the tail of Myo1E, we conducted a yeast two-hybrid screen of a human kidney cDNA library using Myo1E tail fragment containing TH2 and SH3 regions as a bait (Figure 1B). This screen identified a cDNA fragment corresponding to the C-terminal portion of synaptojanin-1, a lipid phosphatase implicated in synaptic vesicle trafficking [20].

Specificity of the two hybrid interaction was verified by examining interaction of synaptojanin-1 with a negative control protein (Lamin C) (Fig. 1C). Synaptojanin-1 contains an N-terminal region homologous to yeast inositol phosphatase Sac1p, a central inositol 5-phosphatase domain, and a C-terminal proline-rich domain (PRD) that is involved in interactions with SH3 domain-containing proteins (Figure 1B). Two isoforms of synaptojanin-1 generated by alternative splicing have been described: a 145 kD isoform expressed primarily in adult neurons and a 170 kD isoform that is more ubiquitously expressed [21]. The two isoforms differ by the presence of several additional proline-rich motifs in the p170 isoform and by distinct membrane-binding properties. The synaptojanin-1 fragment identified in the screen corresponds to the longer, 170 kD, splice form of human synaptojanin-1 and includes a small portion of the inositol 5-phosphatase domain and the entire PRD (Figure 1B).

Synaptojanin-1 and dynamin bind to the SH3 domain of Myo1E

In order to verify Myo1E-synaptojanin-1 interactions, GST-tagged SH3 domain of human Myo1E was used to pull down proteins from rat brain extracts. Synaptojanin-1 bound to GST-SH3 but not to GST alone (Figure 2A). GST-tagged SH3 domain of endophilin-1, a known binding partner of synaptojanin-1 [15], was used as a positive control. In addition to the synaptojanin-1 band, both Myo1E and endophilin pull down reactions contained bands of ~100 kD, the molecular weight of the known endophilin binding protein dynamin [15]. Immunoblot analysis revealed that both dynamin-1 and –2 were present in protein complexes bound to Myo1E and endophilin (Figure 2A). Thus, our data indicate that both long (170 kDa) and short (145 kDa, brain-specific) isoforms of synaptojanin-1, as well as dynamins 1 and 2, interact with Myo1E.

To determine whether interactions of Myo1E SH3 domain with synaptojanin-1 and dynamin were direct and independent of each other, we analyzed binding of synaptojanin-1 and dynamin purified from rat brain to GST-SH3 (Figure 2B). GST-SH3 was able to independently bind to purified synaptojanin-1 and dynamin, confirming that both synaptojanin-1 and dynamin bind directly to the SH3 domain of Myo1E. Binding of synaptojanin-1, dynamin-1, and dynamin-2 to Myo1E SH3 was further confirmed in binding assays, in which GST-SH3 was used to pull down overexpressed human dynamin-1, dynamin-2, or synaptojanin-1 (C-terminal portion of the kidney isoform) or endogenous dynamin-2 from cell lysates (Figure 2C). To verify the importance of the SH3 domain-PRD interaction for Myo1E binding to synaptojanin and dynamin, we introduced a W1089K mutation in the SH3 domain of Myo1E to replace a conserved tryptophan in the hydrophobic groove of the SH3 domain with a positively charged lysine [22]. This mutation disrupted interactions of Myo1E SH3 domain with both synaptojanin-1 and dynamin (Figure 2). Thus, Myo1E interactions with synaptojanin-1 and dynamin involve conserved residues in the SH3 domain and are likely to occur via PRDs in dynamin and synaptojanin-1.

To determine whether Myo1E forms complexes with synaptojanin-1 and dynamin *in vivo*, we immunoprecipitated Myo1E from a synapse-rich fraction of rat brain. Synaptojanin-1 and dynamin are highly expressed at synapses, and we find that Myo1E is enriched over total brain homogenate in this synapse-rich fraction (E.K.O., unpublished observations). Myo1E co-immunoprecipitated with synaptojanin-1 and both dynamin-1 and dynamin-2 (Figure 3).

Myo1E co-localizes with clathrin-coated and dynamin-containing vesicles

Since the binding experiments described above indicated that Myo1E interacts with dynamin and synaptojanin, two proteins that are involved in clathrin-dependent endocytosis, we sought to determine whether Myo1E colocalizes with clathrin associated endocytic structures at the plasma membrane. Previously, TIRF microscopy of live DsRed-clathrin-expressing Swiss 3T3

cells has been successfully used to analyze recruitment of endocytosis-related proteins to clathrin-containing puncta at the plasma membrane (presumably coated pits and newly formed vesicles) [23,24]. TIRF microscopy was used to examine localization of EGFP-tagged Myo1E or Myo1E tail in DsRed-clathrin expressing Swiss 3T3 fibroblasts. DsRed-clathrin and EGFP-Myo1E (or EGFP-Myo1E-tail) localized to puncta on the bottom surface of the cells (Figure 4). In cells co-expressing clathrin and Myo1E, 34.6% of all clathrin-positive puncta contained Myo1E. Interestingly, the degree of co-localization of Myo1E tail with clathrin was higher than that of full-length Myo1E with clathrin (Figure 4), possibly reflecting the fact that in the absence of a functional motor domain Myo1E persists in clathrin-coated structures for prolonged time periods.

Co-localization of Myo1E tail with clathrin was lower in cells expressing Myo1E tail with mutant SH3 domain that does not bind dynamin and synaptojanin (Figure 4). While the presence of the functional SH3 domain was important for proper localization of Myo1E tail, it was not sufficient, since the isolated SH3 domain was mostly diffuse and showed a very low degree of co-localization with clathrin puncta (Figure 4). A tail construct consisting of TH2 and SH3 domains also showed lower degree of co-localization with clathrin than full-length Myo1E tail (Figure 4 A,B). Thus, in addition to the interaction of the SH3 domain with dynamin and/or synaptojanin, the interaction of the positively charged TH1 domain with membrane phospholipids may play an important role in recruitment of Myo1E to clathrin-coated pits and/or vesicles. However, TH1 domain alone was not sufficient for co-localization with clathrin puncta (Figure 4 A,B). In addition, neither EGFP-tagged Myo1A, which possesses only a positively charged TH1 domain but no TH2 or SH3 domains, nor EGFP-tagged Myo1A tail (TH1) localized to clathrin containing puncta (data not shown), further confirming that TH2 and SH3 domains may contribute to proper localization of Myo1E.

We also used TIRF microscopy to determine whether Myo1E is present on dynamin-containing vesicles in live cells. In Swiss3T3 cells transfected with RFP-dynamin-1 and EGFP-Myo1E, Myo1E co-localized with dynamin-containing endocytic structures (Figure 4C). Using immunofluorescence labeling of fixed cells, we also observed co-localization of EGFP-Myo1E-tail and endogenous Myo1E with endogenously expressed dynamin (Figure 5). Only a small fraction of Myo1E-positive puncta was observed to co-localize with dynamin by immunofluorescence; this suggests that it is difficult to detect transient interactions of Myo1E with endocytic vesicles using antibody staining of fixed cells.

These observations confirm that Myo1E interacts *in vivo* with dynamin molecules assembled on endocytic structures at the plasma membrane, such as clathrin-coated pits and budding vesicles. Since synaptojanin-1 is expressed in non-neuronal cells at extremely low levels and, unlike dynamin, its localization in live non-neuronal cells is unknown, we did not examine Myo1E localization in Swiss3T3 or HeLa cells relative to synaptojanin-1 localization.

Expression of Myo1E tail inhibits receptor-mediated endocytosis

To determine whether interactions of Myo1E with its tail-binding partners play a role in endocytosis, we examined uptake of fluorescent transferrin in HeLa cells expressing EGFP-tagged fragments of Myo1E tail, which can act in a dominant-negative fashion by displacing endogenous Myo1E (Figure 6). While almost all control cells exhibited punctate transferrin labeling, ~ 80% of cells expressing Myo1E tail did not take up transferrin (Figure 6B). Presumably, the tail domain displaces endogenous motor by competing with tail-binding partners that may be required for Myo1E localization and/or function in clathrin-mediated endocytosis. Replacement of the conserved tryptophan in the SH3 domain with a lysine (W1089K mutation), which abolishes interactions with synaptojanin and dynamin, reduced the ability of Myo1E tail to inhibit transferrin internalization (Figure 6B), indicating that SH3 domain interactions are important for Myo1E functions. On the other hand, expression of the

isolated SH3 domain did not inhibit transferrin uptake, suggesting that TH1 and/or TH2 domains, which contribute to Myo1E localization to clathrin-coated vesicles, may be necessary to completely displace endogenous Myo1E. Additionally, this observation indicates that inhibition of transferrin uptake by Myo1E DN-tail is not due solely to the SH3 domain sequestering the Myo1E interacting proteins dynamin and synaptojanin but rather due to specific displacement of endogenous Myo1E.

DISCUSSION

Formation of endocytic vesicles at the plasma membrane involves multiple transient interactions between proteins involved in invagination of clathrin-coated pits, vesicle scission, and vesicle uncoating. Assembly of protein complexes during endocytosis relies to a large extent on interactions between SH3 domains and PRDs, which are found in many endocytic proteins. In the present study, we describe binding of two PRD-containing endocytic proteins, dynamin and synaptojanin-1, to the SH3 domain of Myo1E. This interaction was detected both *in vitro*, using pull-downs of purified proteins, and *in vivo*, using immunoprecipitation of protein complexes from synapse-enriched brain extract and immunolocalization of Myo1E and dynamin. Our observation of the interaction between human Myo1E and endocytic proteins suggests that this longtailed myosin may play a role in clathrin-dependent endocytosis. Involvement of longtailed class I myosin in endocytosis has been previously demonstrated for yeast myosins [3,7-9], but not for their mammalian homologs. Recently mouse myosin Myo1f, which is closely related to Myo1E, was shown to regulate presentation of cell adhesion receptors, integrins, on the surface of neutrophils [25], suggesting that long-tailed class I myosins in mammals may contribute to both endo- and exocytosis of cell surface receptors.

Interaction between Myo1E SH3 domain and PRD-containing endocytic proteins may promote recruitment of Myo1E to clathrin-coated structures since an inactivating mutation in the SH3 domain reduced Myo1E localization to clathrin-containing puncta. However, the SH3 domain alone was not sufficient for localization to clathrin-coated vesicles, since removal of the TH1 and TH2 domain abolished vesicular localization. The positively-charged TH1 domain in Myo1E tail may contribute to its localization to the endocytic machinery through interactions with acidic phospholipids or, as has been shown for Myo1A, through interactions with TH-1 binding proteins [19]. The observed role for the SH3 domain in Myo1E localization is reminiscent of findings in budding yeast where SH3 domain of Myo5p is required but not sufficient for polarized localization to cortical patches in the bud [26].

Expression of Myo1E tail in HeLa cells inhibited endocytic uptake of transferrin, which occurs via receptor-mediated endocytosis. This observation suggests that Myo1E tail can act in a dominant-negative manner by displacing endogenous Myo1E, and that disruption of Myo1E interactions with tail-binding proteins inhibits clathrin-dependent endocytosis. An intact SH3 domain and TH1 domain were necessary for the efficient inhibition of transferrin uptake. Thus, both protein-protein interactions mediated by the SH3 domain and membrane binding promoted by the TH1 domain may be important for Myo1E functions in endocytosis. A potential contribution of Myo1E to endocytosis is further substantiated by the observation that mouse Myo1e localizes to the intermicrovillar region of the intestinal brush border, a region characterized by active endocytosis (M.K. and M.S.M., unpublished observations).

There are a number of potential functional roles for the SH3 mediated interaction of Myo1E with synaptojanin-1 and dynamin. Synaptojanin-1 or dynamin may serve as docking sites for Myo1E on the coated pit/vesicle for functions that are independent of the activities of these two proteins. Myo1E may then facilitate coated vesicle formation by remodeling the cortical actin network and/or transporting vesicles away from the plasma membrane and toward the endosomal compartments. Alternatively, Myo1E may regulate dynamin functions during

vesicle scission and/or the phosphatase activity of synaptojanin-1 during vesicle uncoating. Some known examples of regulation of the activity of these proteins by their binding partners include upregulation of GTPase activity of dynamin by binding to SNX9 [27] and activation of phosphatase activity of synaptojanin by binding to the SH3 domain of endophilin [16]. An intriguing possibility is that binding of dynamin and synaptojanin to Myo1E tail may activate motor activity since it has been demonstrated that Myo1E ATPase activity is autoinhibited by its SH3 domain [28]. Disruption of actin cytoskeletal dynamics inhibits fission and internalization of clathrin-coated vesicles [29]; therefore, as an actin-dependent motor localized to clathrin-coated vesicles, Myo1E may play an important role in vesicle formation and internalization.

ACKNOWLEDGEMENTS

We are grateful to the members of De Camilli lab (Yale University Medical School) for the generous gift of dynamin-1 and synaptojanin-1 constructs and antibodies, as well as valuable advice, and to Dr. Wolfhard Almers (OHSU) for a gift of Swiss3T3 cells expressing DsRed-clathrin. We thank members of the Mooseker lab for numerous discussions and critical reading of the manuscript and Dr. Paul Forscher (Yale University), members of the Forscher lab, and Nikon Corporation for help with TIRF microscopy. We would like to thank Vladimir Sirotkin (Yale University) for help with protein purification by FPLC. This work was supported by grants from the NIH (DK-55389, DK-25387 and GM073823; MSM), the Patterson Trust (MSM and David Wells), and the American Heart Association (MK) and by a postdoctoral fellowship from the Arthritis Foundation (MK).

Abbreviations

Myo1, myosin 1; TH, tail homology domain; TIRF, total internal reflection fluorescence microscopy; FBS, fetal bovine serum; EGFP, enhanced green fluorescent protein; RFP, red fluorescent protein; PRD, proline-rich domain.

REFERENCES

[1]. Berg JS, Powell BC, Cheney RE. A millennial myosin census. Mol Biol Cell 2001;12:780–94. [PubMed: 11294886]

[2]. Mooseker MS, Cheney RE. Unconventional myosins. Annu Rev Cell Dev Biol 1995;11:633–75. [PubMed: 8689571]

[3]. Geli MI, Riezman H. Role of type I myosins in receptor-mediated endocytosis in yeast. Science 1996;272:533–5. [PubMed: 8614799]

[4]. Evangelista M, et al. A role for myosin-I in actin assembly through interactions with Vrp1p, Bee1p, and the Arp2/3 complex. J Cell Biol 2000;148:353–62. [PubMed: 10648568]

[5]. Lechler T, Shevchenko A, Li R. Direct involvement of yeast type I myosins in Cdc42-dependent actin polymerization. J Cell Biol 2000;148:363–73. [PubMed: 10648569]

[6]. Jung G, Remmert K, Wu X, Volosky JM, Hammer JA 3rd. The Dictyostelium CARMIL protein links capping protein and the Arp2/3 complex to type I myosins through their SH3 domains. J Cell Biol 2001;153:1479–97. [PubMed: 11425877]

[7]. Sirotkin V, Beltzner CC, Marchand JB, Pollard TD. Interactions of WASp, myosin-I, and verprolin with Arp2/3 complex during actin patch assembly in fission yeast. J Cell Biol 2005;170:637–48. [PubMed: 16087707]

[8]. Sun Y, Martin AC, Drubin DG. Endocytic internalization in budding yeast requires coordinated actin nucleation and myosin motor activity. Dev Cell 2006;11:33–46. [PubMed: 16824951]

[9]. Engqvist-Goldstein AE, Drubin DG. Actin assembly and endocytosis: from yeast to mammals. Annu Rev Cell Dev Biol 2003;19:287–332. [PubMed: 14570572]

[10]. Baines IC, Brzeska H, Korn ED. Differential localization of Acanthamoeba myosin I isoforms. J Cell Biol 1992;119:1193–203. [PubMed: 1447297]

[11]. Jung G, Wu X, Hammer JA 3rd. Dictyostelium mutants lacking multiple classic myosin I isoforms reveal combinations of shared and distinct functions. J Cell Biol 1996;133:305–23. [PubMed: 8609164]

[12]. Bement WM, Wirth JA, Mooseker MS. Cloning and mRNA expression of human unconventional myosin-IC. A homologue of amoeboid myosins-I with a single IQ motif and an SH3 domain. J Mol Biol 1994;243:356–63. [PubMed: 7932763]

[13]. Swanson JA, Johnson MT, Beningo K, Post P, Mooseker M, Araki N. A contractile activity that closes phagosomes in macrophages. J Cell Sci 1999;112(Pt 3):307–16. [PubMed: 9885284]

[14]. Skowron JF, Bement WM, Mooseker MS. Human brush border myosin-I and myosin-Ic expression in human intestine and Caco-2BBe cells. Cell Motil Cytoskeleton 1998;41:308–24. [PubMed: 9858156]

[15]. Ringstad N, Nemoto Y, De Camilli P. The SH3p4/Sh3p8/SH3p13 protein family: binding partners for synaptojanin and dynamin via a Grb2-like Src homology 3 domain. Proc Natl Acad Sci U S A 1997;94:8569–74. [PubMed: 9238017]

[16]. Lee SY, Wenk MR, Kim Y, Nairn AC, De Camilli P. Regulation of synaptojanin 1 by cyclin-dependent kinase 5 at synapses. Proc Natl Acad Sci U S A 2004;101:546–51. [PubMed: 14704270]

[17]. Naisbitt S, Valtschanoff J, Allison DW, Sala C, Kim E, Craig AM, Weinberg RJ, Sheng M. Interaction of the postsynaptic density-95/guanylate kinase domain-associated protein complex with a light chain of myosin-V and dynein. J Neurosci 2000;20:4524–34. [PubMed: 10844022]

[18]. Ceresa BP, Lotscher M, Schmid SL. Receptor and membrane recycling can occur with unaltered efficiency despite dramatic Rab5(q79l)-induced changes in endosome geometry. J Biol Chem 2001;276:9649–54. [PubMed: 11136733]

[19]. Tyska MJ, Mooseker MS. A role for myosin-1A in the localization of a brush border disaccharidase. J Cell Biol 2004;165:395–405. [PubMed: 15138292]

[20]. McPherson PS, et al. A presynaptic inositol-5-phosphatase. Nature 1996;379:353–7. [PubMed: 8552192]

[21]. Ramjaun AR, McPherson PS. Tissue-specific alternative splicing generates two synaptojanin isoforms with differential membrane binding properties. J Biol Chem 1996;271:24856–61. [PubMed: 8798761]

[22]. Tanaka M, Gupta R, Mayer BJ. Differential inhibition of signaling pathways by dominant-negative SH2/SH3 adapter proteins. Mol Cell Biol 1995;15:6829–37. [PubMed: 8524249]

[23]. Merrifield CJ, Feldman ME, Wan L, Almers W. Imaging actin and dynamin recruitment during invagination of single clathrin-coated pits. Nat Cell Biol 2002;4:691–8. [PubMed: 12198492]

[24]. Merrifield CJ, Qualmann B, Kessels MM, Almers W. Neural Wiskott Aldrich Syndrome Protein (N-WASP) and the Arp2/3 complex are recruited to sites of clathrin-mediated endocytosis in cultured fibroblasts. Eur J Cell Biol 2004;83:13–8. [PubMed: 15085951]

[25]. Kim SV, et al. Modulation of cell adhesion and motility in the immune system by Myo1f. Science 2006;314:136–9. [PubMed: 17023661]

[26]. Anderson BL, Boldogh I, Evangelista M, Boone C, Greene LA, Pon LA. The Src homology domain 3 (SH3) of a yeast type I myosin, Myo5p, binds to verprolin and is required for targeting to sites of actin polarization. J Cell Biol 1998;141:1357–70. [PubMed: 9628892]

[27]. Soulet F, Yarar D, Leonard M, Schmid SL. SNX9 regulates dynamin assembly and is required for efficient clathrin-mediated endocytosis. Mol Biol Cell 2005;16:2058–67. [PubMed: 15703209]

[28]. Stoffler HE, Bahler M. The ATPase activity of Myr3, a rat myosin I, is allosterically inhibited by its own tail domain and by Ca2+ binding to its light chain calmodulin. J Biol Chem 1998;273:14605–11. [PubMed: 9603977]

[29]. Yarar D, Waterman-Storer CM, Schmid SL. A dynamic actin cytoskeleton functions at multiple stages of clathrin-mediated endocytosis. Mol Biol Cell 2005;16:964–75. [PubMed: 15601897]

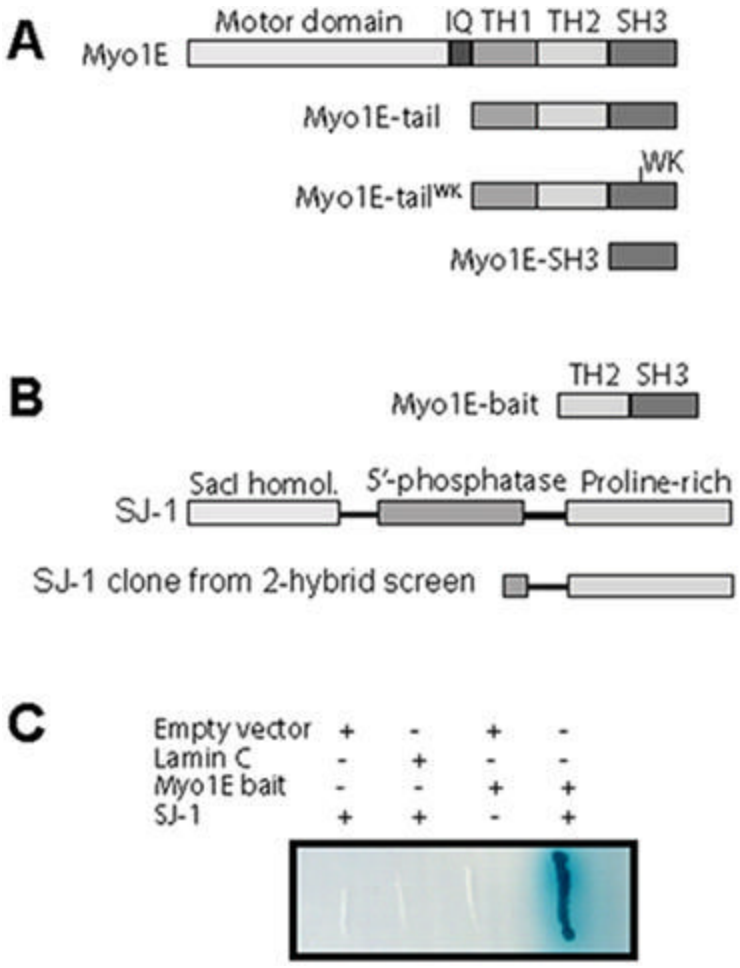

Figure 1.

Myo1E tail structure and identification of tail-binding proteins using yeast two-hybrid screen.

A. The domain structure of Myo1E and the tail constructs used to investigate Myo1E localization. Myo1E heavy chain is composed of an N-terminal motor domain, a neck domain with a single IQ light chain binding motif, and a tail domain. Myo1E tail consists of a positively charged TH1 domain, a proline-rich TH2, and an SH3 (TH3) domain [2].

B. Myo1E construct used as a bait for the yeast two-hybrid screening consists of TH2 and SH3 domain. Synaptojanin-1 (SJ-1) contains two phosphatase domains (Sac1-homology and inositol-5-phopshatase) and a C-terminal PRD. Synaptojanin-1 fragment isolated in the yeast two hybrid screen includes a portion of the inositol 5-phosphatase domain and the PRD.

C. Interaction of Myo1E with SJ-1 in a yeast two-hybrid assay. Yeast clone containing both Myo1E bait construct and SJ-1 construct exhibits signs of a positive interaction: the ability to grow on the nutrient-deficient medium and development of blue color due to ß-galactosidase reaction. Negative controls (Myo1E bait plus empty vector, SJ-1 construct plus empty vector, SJ-1 construct plus non-interacting protein (Lamin C)) do not grow on the nutrient-deficient medium.

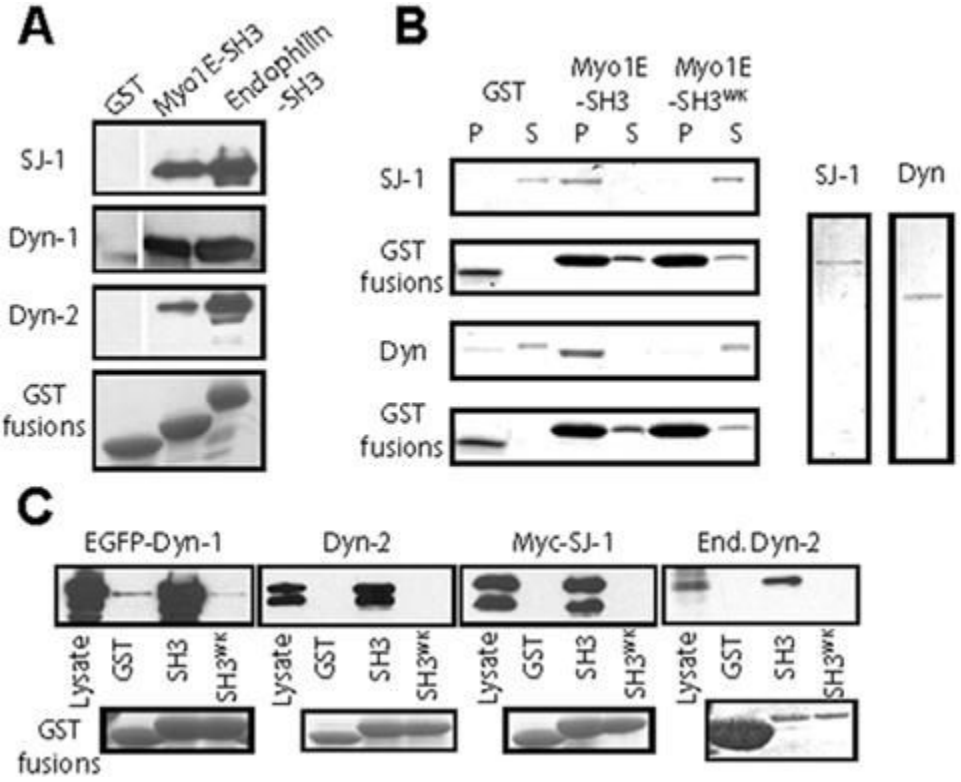

Figure 2.
Interaction of Myo1E with synaptojanin-1 and dynamin.

A. Myo1E binding proteins from rat brain extracts. Immunoblot analysis indicates that both GST-tagged Myo1E SH3 and endophilin-SH3 but not GST alone bind synaptojanin-1 (SJ-1), dynamin-1, and dynamin-2 (Dyn-1,2). A Coomassie stained gel showing the amount of GST fusion proteins used for pulldowns is shown in the lower panel (GST fusions).

B. Binding of purified synaptojanin-1 and dynamin to Myo1E SH3 domain. SDS-PAGE of glutathione-bead pellet (P) and supernatant (S) fractions followed by Coomassie staining indicates that GST-tagged Myo1E SH3 but not mutant SH3 or GST bind purified synaptojanin-1 and dynamin. Note that mobility shift of dynamin band in lane 3 (SH3 pellet) is a gel artifact caused by the difference in total protein load between the lanes. Right-hand panels show Coomassie stained gels of the purified synaptojanin-1 and dynamin preparations used.

C. Binding of synaptojanin-1, dynamin-1, and dynamin-2 expressed in cultured cells to Myo1E SH3. Cos-1 cells transfected with EGFP-tagged dynamin-1 or myc-tagged synaptojanin-1 (partial clone isolated from the kidney cDNA library), HeLa cells transfected with untagged dynamin-2 or non-transfected HeLa cells were lysed and cell lysates were incubated with GST-tagged proteins as indicated. Immunoblots indicated that overexpressed synaptojanin-1 and dynamin-1 and -2 as well as endogenous dynamin-2 (End. Dyn-2) from HeLa lysate bound to GST-SH3 but not pure GST or mutant SH3 ($SH3^{WK}$). Lower panels show Coomassie stained gels of the GST fusions used.

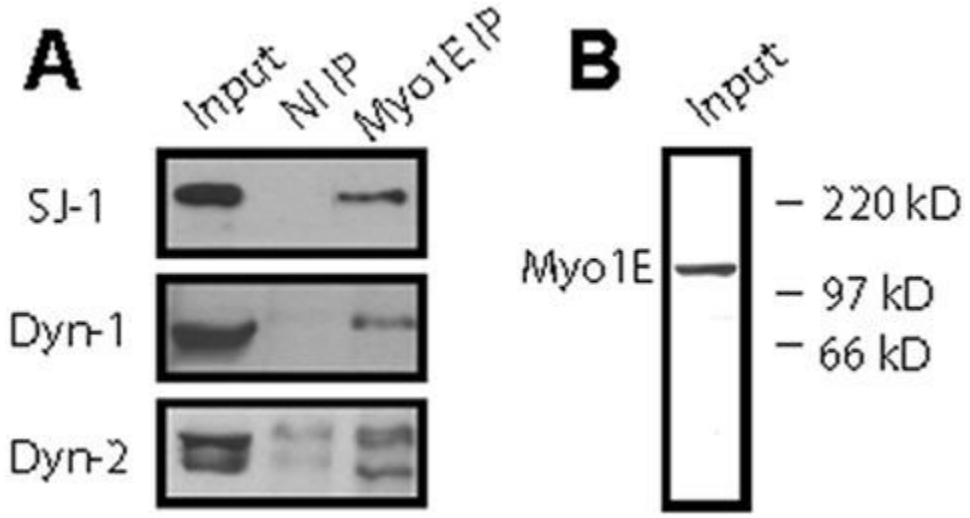

Figure 3.
Immunoprecipitation of Myo1E-binding proteins from synapse-enriched rat brain extract.

A. Immunoblot analysis indicated that synaptojanin-1, dynamin-1 and -2 were present in Myo1E immunoprecipitates but not in non-immune immunoprecipitates.

B. Anti-Myo1E antibody used for immunoprecipitation recognized a single band in the synapse-enriched rat brain preparation. Positions of molecular weight markers are shown on the right.

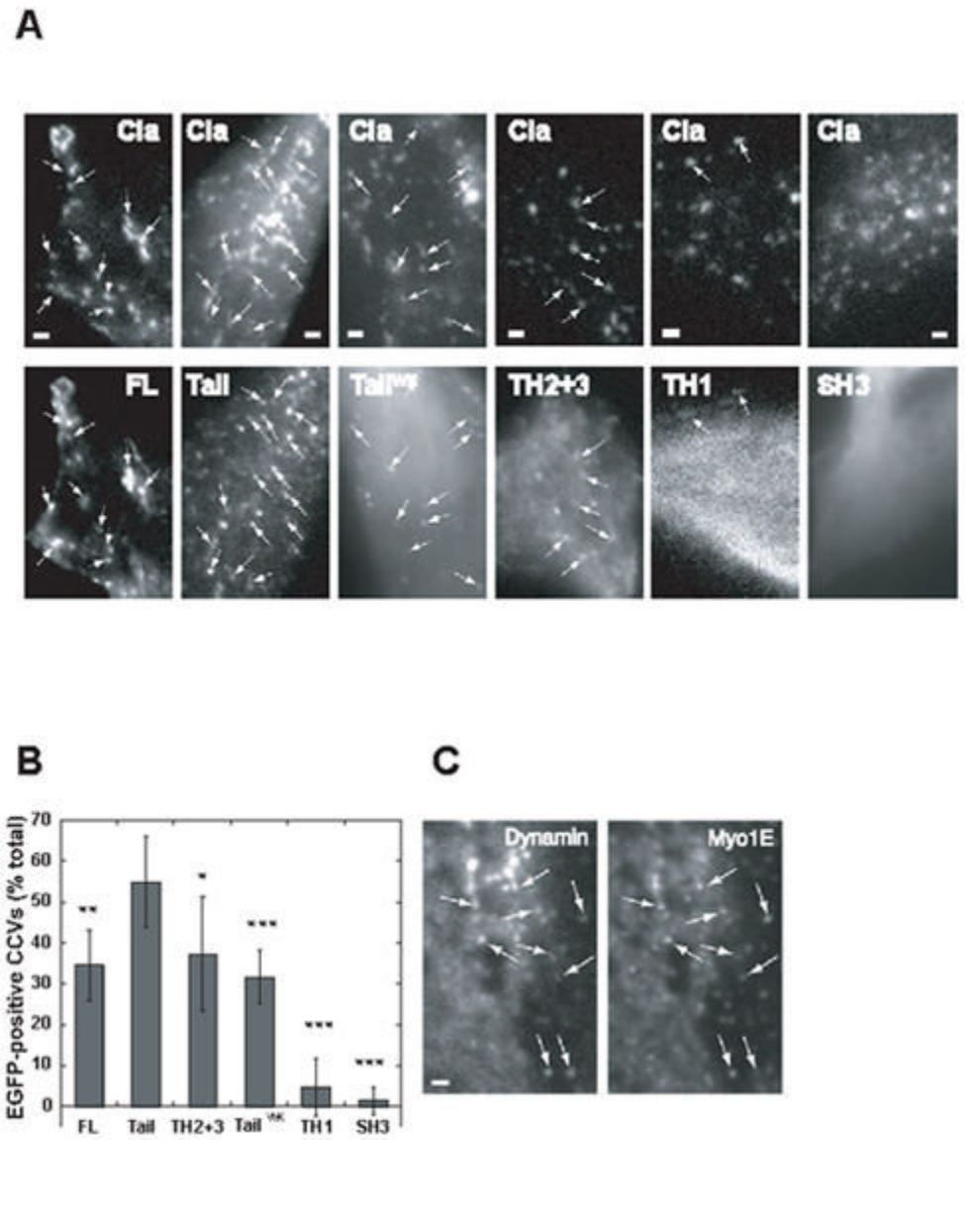

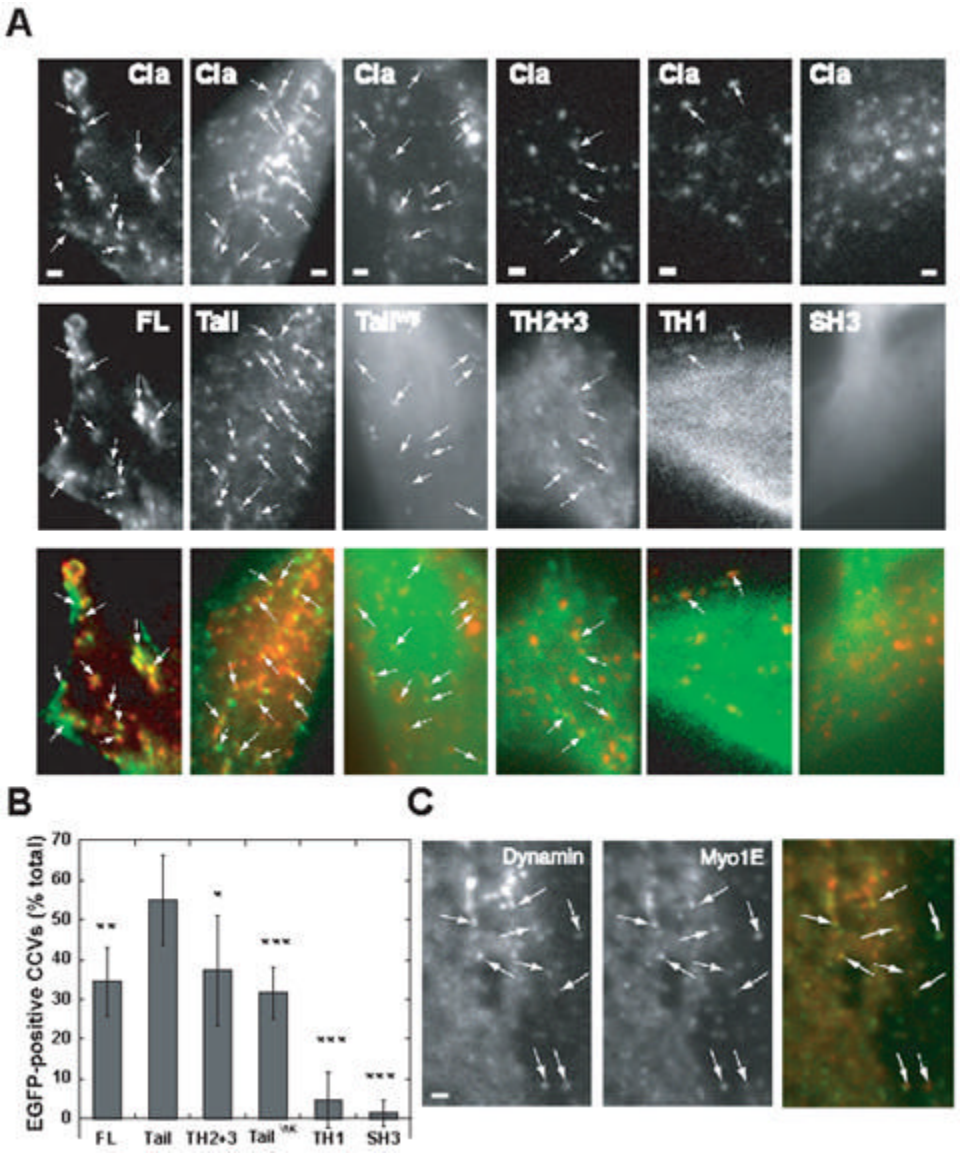

Figure 4.

Co-localization of Myo1E and Myo1E tail constructs with clathrin- and dynamin-labeled vesicles in live Swiss3T3 cells.

A. Swiss3T3 fibroblasts stably expressing DsRed-clathrin (Cla) were transfected with EGFP-tagged Myo1E, Myo1E tail containing all three tail homology regions (TH1, TH2, SH3), mutant tail (tail^{WK}) or partial tail constructs (TH1 only, TH2+SH3 (TH2 +3), SH3 only) and imaged using TIRF microscopy. Vesicles labeled with both green and red fluorescent proteins are marked by arrows. Scale bar - 1 μm.

B. Frequency of colocalization of various Myo1E constructs with clathrin-positive puncta. Percentage of clathrin-coated vesicles (CCVs) labeled with EGFP-tagged Myo1E constructs was determined as described in Materials and Methods. Numbers shown represent average percentages+/-SD for 5 cells for Myo1E, tail^{WK}, and SH3 constructs, 7 cells for TH2+3 and TH1, and 10 cells for Myo1E tail. Average percent colocalization for each construct was compared with the average percent colocalization for Myo1E tail using t-test. * - P< 0.05, ** - P<0.005, *** - P<0.001.

C. Colocalization of EGFP-Myo1E and mRFP-dynamin-1 in Swiss3T3 cells by TIRF microscopy. Arrows indicate fluorescent puncta that contain both EGFP-Myo1E and dynamin. Scale bar - 1 um.

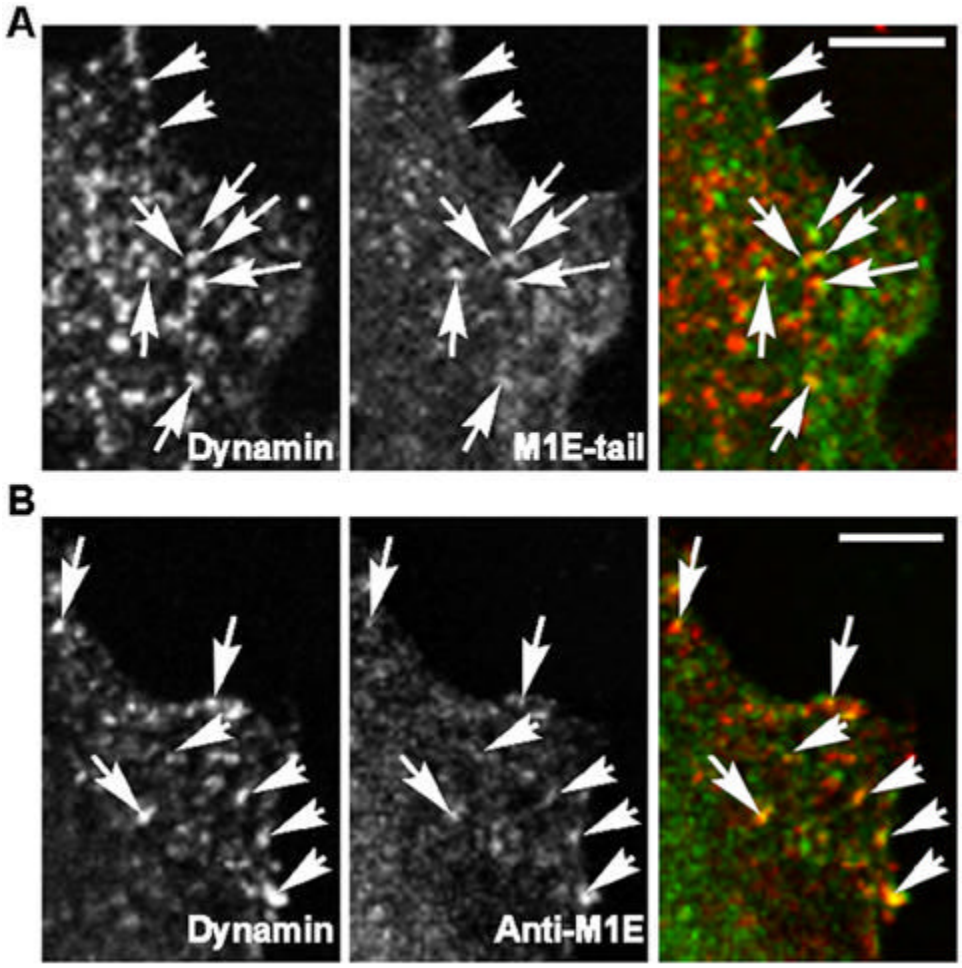

Figure 5.

Co-localization of Myo1E-tail or endogenous Myo1E with endogenous dynamin in HeLa and Swiss 3T3 cells. HeLa cells transfected with EGFP-Myo1E-tail(A) or untransfected Sw3T3 cells (B) were fixed, stained with antibodies against dynamin(A) or dynamin and Myo1E (B), and imaged using confocal microscopy. Arrows point to vesicles that contain both Myo1E and dynamin. Scale bar - 5 μm.

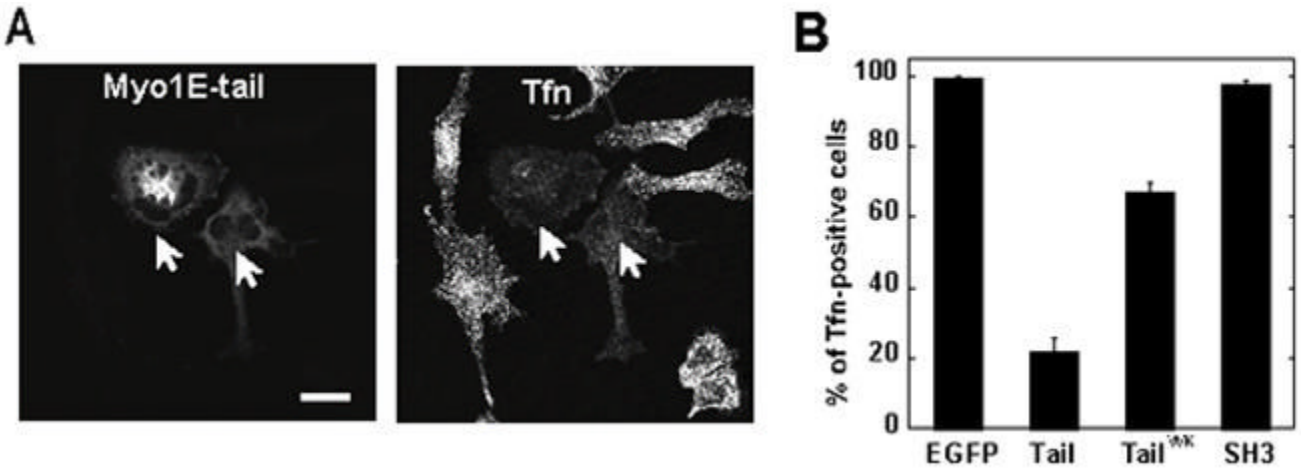

Figure 6.
Inhibition of transferrin uptake by Myo1E tail construct.

A. Transferrin (Tfn) uptake in EGFP-Myo1E tail-transfected HeLa cells. Cells expressing Myo1E tail (arrows) did not exhibit punctate transferrin labeling. Scale bar - 20 μm.

B. Quantitative analysis of transferrin endocytosis in HeLa cells. Cells transfected with various DNA constructs were allowed to take up fluorescent transferrin and processed as in A. Percent of transfected cells exhibiting punctate transferrin labeling was determined from three independent experiments (N>/=100 cells for each experiment, error bars=SD).